

Optimizing Heat Transfer Characteristics on the Performance of Photovoltaic/Thermal Collector Using Various Absorber Design

Ali Mohammed Hayder

Technical Institute of Najaf, Al-Furat Al-Awsat Technical University, Al-Najaf, Iraq.

Abstract - To accomplish extraordinary efficiency besides significant extents of command also heat since PV/T schemes, PV cells should be refrigerated, predominantly in parts using broiling and steamy climate. CFD Simulation revision has been investigated to optimize the hotness allocation individualities of absorber design using FVM. Four different absorber configurations (round, square and rectangular) have been demonstrated besides inspected to generate broiling aquatic with current. The results show that the Rectangular [$w = 25 \text{ mm}$, $d = 15 \text{ mm}$] absorber collector generates a pooled PV/T efficiency of 73.4 % with electrical competence of 11.2 %. Moreover, the round absorber antenna engenders a collective PV/T competence of 54.43 % besides electrical proficiency of 9.35 %. The proficiency of the PV/T scheme should be enhanced additional via settled the sides among the absorber with solar sheet (PV segment).

Key words: Absorber design, Photovoltaic/Current, Thermal, Verve.

INTRODUCTION

A mixture photovoltaic thermal (PV/T) scheme, in the heat starting the PV sheet is detached via a waged fluid, can concurrently renovate lunar energy hooked on electrical in addition to current energy. Paralleled with discrete PV or current schemes, the mixture method has numerous benefits, counting great entire energy alteration efficiency, stumpy cost, also minor installation areas (Cox Iii and Raghuraman 1985, Jedsadaratanachai and Boonloi 2018, Ndlovu and Moitsheki 2018). Hybrid(mixture) thermal energy schemes are hybrid power schemes that cartel astral energy from a photovoltaic scheme with alternative cradle to engender electrical vitality (Sok, Zhuo et al. 2010). The photovoltaic and diesel mixture scheme is one of the public brands that combine photovoltaic sheets besides diesel initiators, subsequently photovoltaic sheets do not have a ancillary cost also have the benefit in the gridiron. The energy manufactured via this organization (Duffie and Beckman 2013, Zarita and Hachemi 2018, Sapit and Pahat 2019) is supplementary constant and a lesser amount of impulsive than additional two-factor sub schemes (Zondag 2008, Zhong and Ling 2020). While (Joshi, Tiwari et al. 2009) deliberate and equaled two PV arrangements specifically; classical (I) glass-to-tedlar besides to classical (II) glass-to-glass. To carry out investigational and mathematical investigations (Mbewe, Card et al. 1985, Chow 2003, Tripanagnostopoulos 2007). Literature showed that the PV/T expertise has an essential downside of fabricating junior proficiencies compared to their discrete parts, owing to lower absorption constant and sophisticated current struggle (Sok, Zhuo et al. 2010). Meanwhile, study the optimum diameter and configurations prominent to grander heat allocation features into PV/T collectors (Abbud, Balla et al. 2019). Therefore, enhancing heat transfer using different designs is implemented in this work. The present work is a simulation study using CFD-ANSYS to investigate the effects of optimum absorber design (Zondag, Jong et al. 2001) by using water on the PV/T's collector performance to determine the maximum enhancement that can be achieved (Takashima, Tanaka et al. 1994, Skoplaki and Palyvos 2009, Al-Shamani, Yazdi et al. 2014).

METHODOLOGY

1. Governing Reckonings

The governing reckonings (endurance, vitality) requisite is regular to widespread CFD inquiry of the PVT amasser. The singularity lower than consideration was ruled via the firm 3D computational realm of the endurance, stage-be in the region of incompressible Navier–Stokes reckonings, besides vitality reckoning. In the Cartesian tensor scheme, these reckonings may possibly be inscribed as (Eiamsa-ard and Promvong 2008).

Continuity reckoning:

$$\frac{\partial}{\partial x_i}(\rho u_i) = 0 \quad (1)$$

Momentum reckoning:

$$\frac{\partial(\rho u_i u_j)}{\partial x_i} = -\frac{\partial p}{\partial x_j} + \frac{\partial}{\partial x_j} \left[\mu \left(\frac{\partial u_i}{\partial x_j} + \frac{\partial u_j}{\partial x_i} \right) \right] + \frac{\partial}{\partial x_j} (-\rho \overline{u_i' u_j'}) \quad (\text{Error! No text of specified style in document.2})$$

Energy reckoning:

$$\frac{\partial}{\partial x_i} (\rho u_i T) = \frac{\partial}{\partial x_j} \left((\Gamma + \Gamma_t) \frac{\partial T}{\partial x_j} \right) \quad (\text{Error! No text of specified style in document.3})$$

Where Γ and Γ_t are molecular thermal diffusivity and turbulent thermal diffusivity, respectively, and are expressed as follows:

$$\Gamma = \frac{\mu}{Pr}, \Gamma_t = \frac{\mu_t}{Pr_t} \quad (\text{Error! No text of specified style in document.4})$$

The turbulent viscosity term μ_t should be computed from an appropriate turbulence model. Turbulent viscosity is expressed as follows:

$$\mu_t = \rho C_\mu \frac{k^2}{2} \quad (5)$$

2. Energy Exploration of PV/T Gatherer

PV effectiveness diminutions once the fever of the chambers growths. The effectiveness to the photovoltaic cells hinge on on fever (Coventry 2005). Promote, the routine of PV/T Gatherer canister be portrayed via combination of adeptness manifestation. It is excluded of the current PVT proficiency η_{th} besides to electrical PVT effectiveness η_{el} , that is habitually excludes the quotient of the beneficial current achievement besides to electrical achievement of the scheme to occasion of lunar irradiance on the gatherer's crack surrounded by a precise stretch or dated. As given away in Reckoning 1, the overall PVT effectiveness of $\eta_{overall}$ is used to assess the global concert in scheme (Sok E et al 2010).

$$\eta_{overall} = \eta_{th} + \eta_{pv} \quad (6)$$

Thus, the descent of the effectiveness limitations constructed on the Hottel-Whillier reckoning was used. The thermal PVT efficiency (η_{th}) can be calculated via the Reckoning (2):

$$\eta_{th} = \frac{Q_u}{Q_{in}} \quad (7)$$

Using Reckoning (2), the useful heat placid (Q_u) via the aquatic in rapports of its fever rise can be traveled further via Reckoning (3):

$$Q_u = \dot{m} C_p (T_o - T_i) \quad (8)$$

The metamorphosis flanked by current emotion injuries besides absorber stellar irradiance was identified via Hottel-Whillier reckonings then the energy steadiness reckoning for the Gatherer is identifying as in Reckoning (4):

$$Q_u = A_c F_R \times [S(\tau\alpha) - U_L(T_i - T_a)] \quad (9)$$

At Reckoning (4), the astrophysical irradiance riveted via a Gatherer each part of absorber S is the same to the alteration flanked by the incidents of solar irradiances and ocular finds. The S can be identified using Reckoning (5):

$$S = (\tau\alpha)_{pv} G_T \quad (10)$$

The emotion elimination competence influence (F_R) can be planned by way of in Reckoning (6):

$$F_R = \frac{n\&C_p}{A_c U_L} \times \left[1 - \exp\left(-\frac{A_c U_L F'}{n\&C_p}\right) \right] \quad (11)$$

The corrected fin effectiveness (F') is intended via expending the subsequent reckoning:

$$F' = \frac{\frac{1}{U_L}}{W \left[\frac{1}{U_L (D + (W - D)F)} + \frac{1}{c_b} + \frac{1}{\pi D_i h_{fi}} \right]} \quad (12)$$

Consequently, the effectiveness influence F bowl be designed via Reckoning (7):

$$F = \frac{\tanh\left[M\left(\frac{W - D}{2}\right)\right]}{M\left(\frac{W - D}{2}\right)} \quad (13)$$

$$M = \sqrt{\frac{U_L}{(K_{abs} L_{abs}) + (K_{pv} + L_{pv})}} \quad (14)$$

$$\eta_{th} = F_R (\tau\alpha) - F_R U_L \left(\frac{T_i - T_a}{G_T}\right) \quad (15)$$

The temperature-dependent electrical efficiency of the PV panel (η_{el}) is expressed as follows (Tiwari and Sodha 2006):

$$\eta_{el} = \eta_r (1 - \chi (T_{pm} - T_r)) \quad (16)$$

Wherever η_{el} is the electrical effectiveness, η_r is the orientation competence of the PV sheet ($\eta_r = 0.14$), χ is the fever constant ($0.0045 \text{ } ^\circ\text{C}^{-1}$), T_{pm} is the hotness of the astral chambers (K), and T_r is the orientation hotness.

3. Intention Alignments of the Absorber

As the PV prison cell in PV segment is bare to an emission, they engender electricity however absorbing hotness, triggering the absorber to escalation its hotness. For the duration of this stage, the base fluid momentary enter in the absorber ducts is passionate as of the commerce inferior to the PV segment. Schematics of PV/T collectors were used for the geometrical model. Study the different absorber configuration as shown in Table 1 below.

TABLE 1
PV/T ABSORBER DESIGN AND CONFIGURATIONS

Round tube	Square		Rectangular		
Case 1	d, mm	Case 2	d, mm	Case 3	w, mm
	10		10		15
	12.5		12.5		17.5
Optimum Round	15	Optimum d	15	Optimum d	20
	17.5		17.5		22.5
	20		20		25

4. Borderline Surroundings

Applicable borderline surroundings are emphasized on CFD province as the astronomy of the delinquent. Creek limit surroundings are quantified as rapidity cove circumstances. The pressure outlet boundary ailment is functional at the channel. Barricade borderline surroundings are secondhand to dilemma fluid besides hard districts. The border in the middle of the base fluid with absorber hose is branded as the hedge with attached state to replace hotness exchange as of the absorber hose to base fluid.

5. Methods

CFD-ANSYS virtual reality apparatus, laid-back with energy equilibrium reckonings, are going to be used to determine the heat transfer enhancement. Figure 1 illuminates the wedge graph of the theoretical study (Al-Shamani, Mat et al. 2016) evolution methodology.

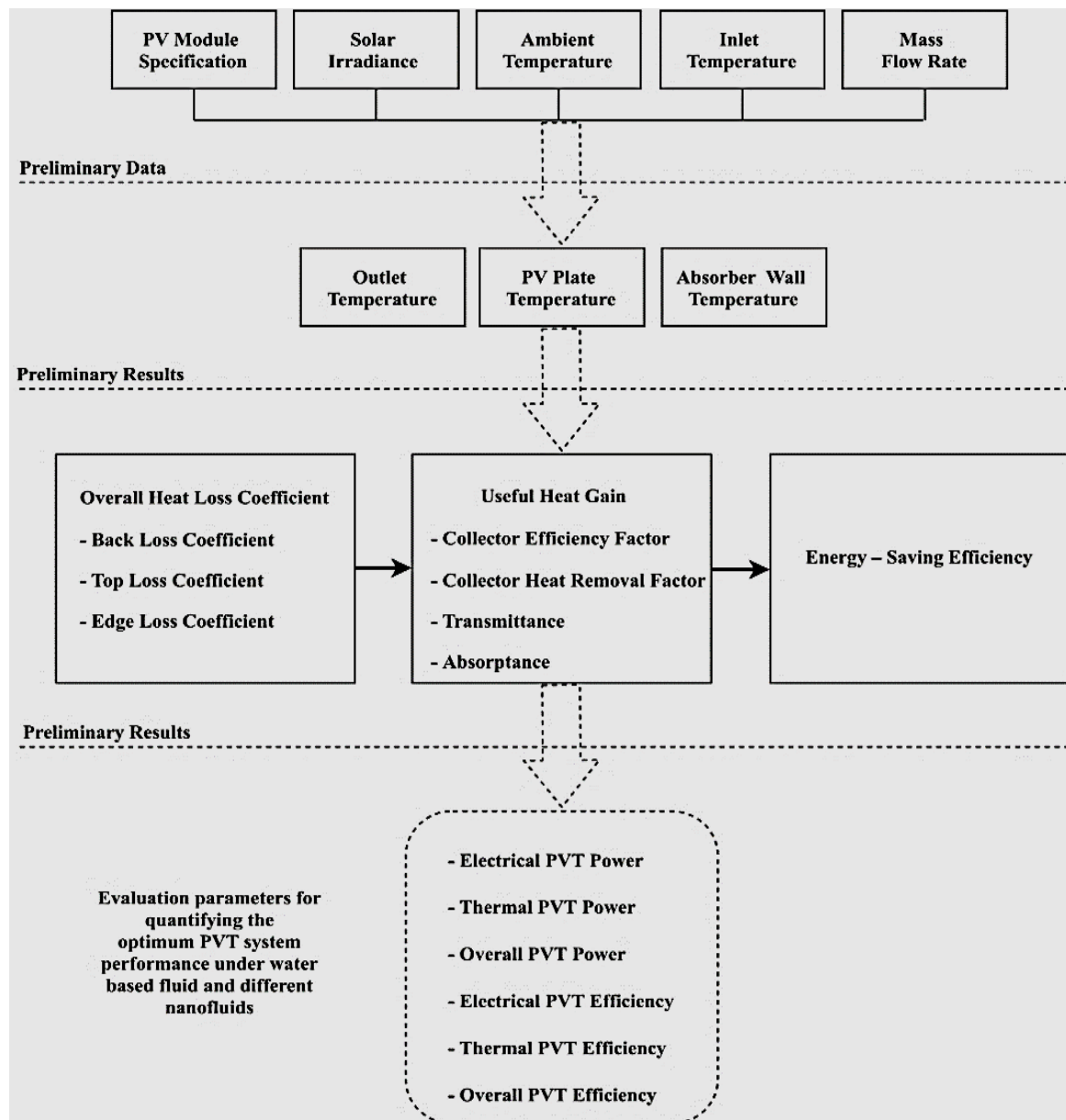


FIGURE 1
CHUNK ILLUSTRATION OF THE THEORETICAL STUDY PROGRESSION APPROACH

RESULTS AND OBSERVATION

1. Code Authentication

Code Authentication is actual essential stage in any statistical effort in order to safeguard that they are endorsed statistical cryptograph with other erstwhile grind, and it is equipped for tracks. It is not merely central to acquire a extraordinary faithfulness of any statistical code, but besides to acquire a restored sympathetic of the aptitudes and restrictions. (Fudholi, Sopian et al. 2014) was particular to be undisputable of code validation. The appraisal of the CFD validation results thermal, electrical and overall efficiencies are validation as shown in Figure 2.

Figures 2 shows the (electrical, thermal, overall) PV/T efficiency, it is vibrant to see that the effectiveness growths with increased the mass movement degree. The CFD results almost close the A. Fudholi results. The overall effectiveness of A. Fudholi results for spiral flow absorber was 58 % - 68.4 %.

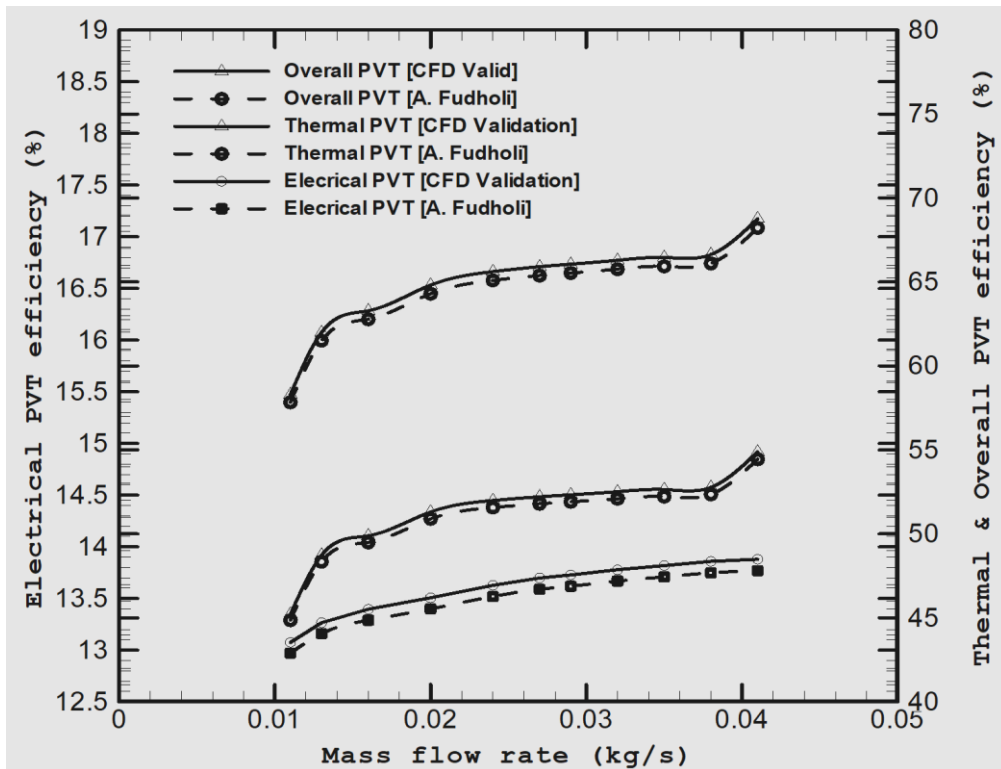


FIGURE 2

ELECTRICAL, CURRENT AND INCLUSIVE PV/T EFFECTIVENESS IN COMPETITION WITH MASS MOVEMENT RATE FOR THE CFD VALIDATION RESULTS COMPARE WITH THE RESULTS OF FUDHOLI (FUDHOLI, SOPIAN ET AL. 2014)

2. Grating Impartiality Test

The grating cohort theaters a vital essence in any effectiveness measurements. A accurate mesh provides us with estimated elucidations to the restricted variance reckonings. As shown clearly in Figure 3, the mesh for the absorber Quadrangular channel [$d = 20\text{ mm}$], $\dot{m} = 0.068\text{ kg/s}$. Entirely mesh expressions are charity to intrigue the callous PV/T salver fever on the equivalent XY intrigue. The discretization grating is regulated and constant.

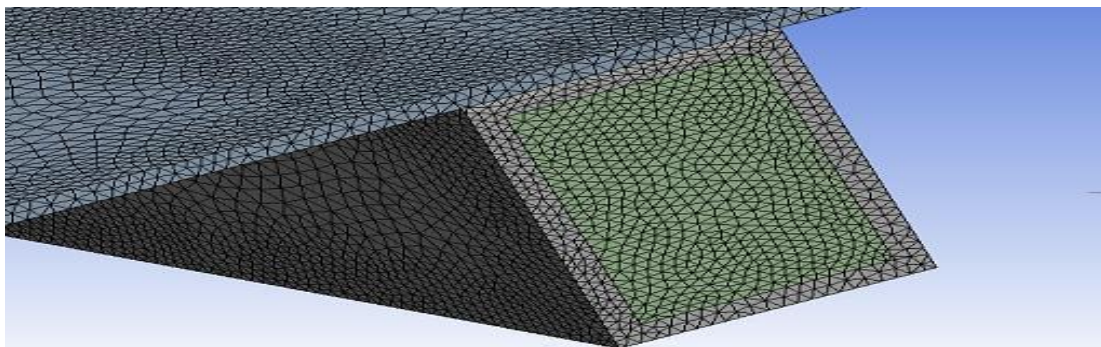


FIGURE 3

CFD MESHING OF ABSORBER SQUARE CYLINDER [$D = 20\text{ mm}$]

As shown clearly in Figure 4 that entirely the five mesh aspects (100411, 1136229, 1229870, 1743827 and 2015091) have related grades of callous PV/T salver malaise. Conversely, slightly unique of the five faces can be castoff. In that situation, mesh faces (1004111) also mean PV/T bowl hotness ($54.32\text{ }^\circ\text{C}$) is secondhand as it is the superlative in relations of mutually the truth in addition to computational stage.

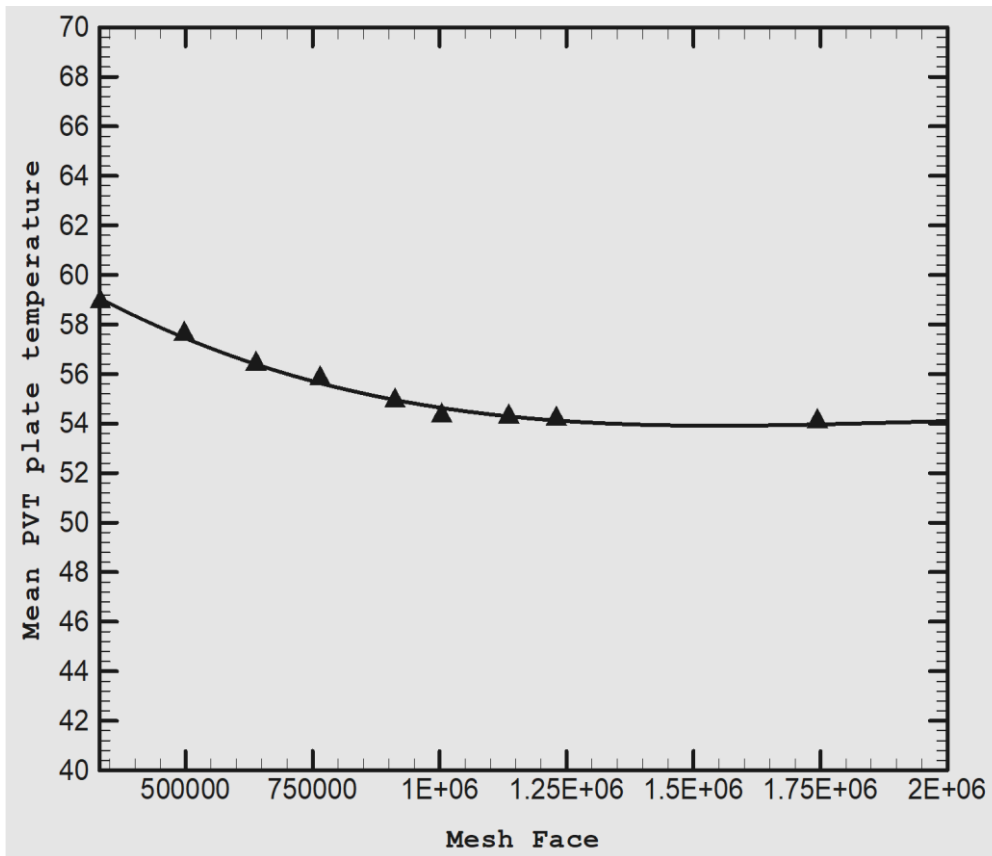


FIGURE 4
GRID INDEPENDENT TEST

3. Predicting of Absorber Dimensions for Optimum Reduction of Mean PV/T Module Temperature

In this round of analysis, the optimum absorber dimensions (Round $[d]$, Square $[d]$ and Square $[w, d]$) that can realize the best PV/T module temperature reduction will be determined. Figure 5 to Figure 7 illustrate the effect of absorber dimensions on the callous PV/T segment fever at altered solar emission levels ($400 \text{ W/m}^2 - 1000 \text{ W/m}^2$) and mass current rate $\dot{m} = 0.068 \text{ kg/s}$. Figure 5 shown the influence of Round tube dimensions on the mean PV/T module temperature (T_{pm}), it is clear to see the when increased the tube diameter $[d]$ the T_{pm} decreases and it is be almost constant at Round tube $[d = 20 \text{ mm}]$ therefore form all these dimensions $[d = 10 \text{ mm} - 27.5 \text{ mm}]$ will select the Round tube $[d = 15 \text{ mm}]$ and $[d = 20 \text{ mm}]$ for simulation and experimental study.

Figure 6 shown the effect of Square tube dimensions on the mean PV/T module temperature (T_{pm}), it is clear to see the when increased the tube diameter $[d]$ the T_{pm} decrease and it is be almost constant at Square tube $[d = 15 \text{ mm}]$ decreased slightly till $[d = 20 \text{ mm}]$ therefore form all these dimensions $[d = 10 \text{ mm} - 25 \text{ mm}]$ will select the Square tube $[d = 20 \text{ mm}]$ for simulation and experimental study. Regarding to Figure 6 the optimum dimensions of Square tube $[d = 15 \text{ mm}]$ select this diameter to be the depth of Square tube and do the CFD test to get the optimum width of the tube. Figure 7 shown the effect of Square tube width on the mean PV/T module temperature (T_{pm}), it is clear to see the when increased the tube width $[w]$ the T_{pm} decreases and it is be almost constant at Square tube $[w = 25 \text{ mm}]$ therefore form all these dimensions $[w = 15 \text{ mm} - 30 \text{ mm}]$ will select the Square tube $[w=25 \text{ mm}]$ for simulation and experimental study.

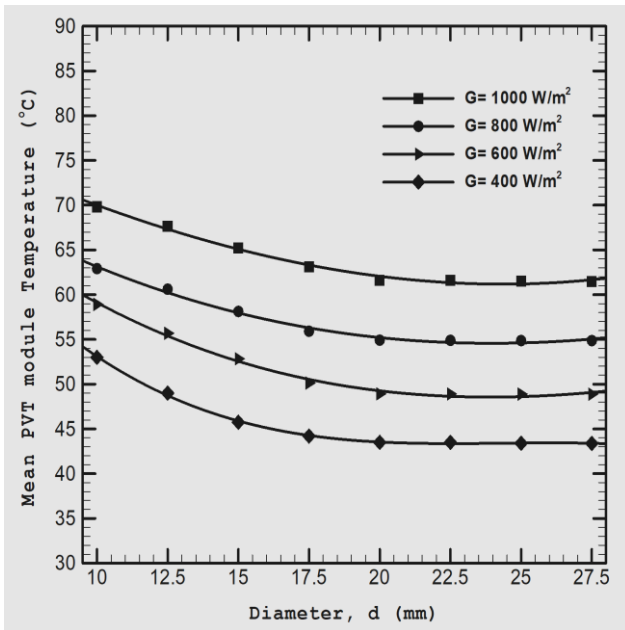


FIGURE 5

T_{PM} VERSUS THE PVT ABSORBER DIMENSIONS (ROUND TUBE) AT ALTERED SOLAR IRRADIANCE BESIDES MASS FLOWRATE $\dot{m} = 0.068 \text{ KG/S}$

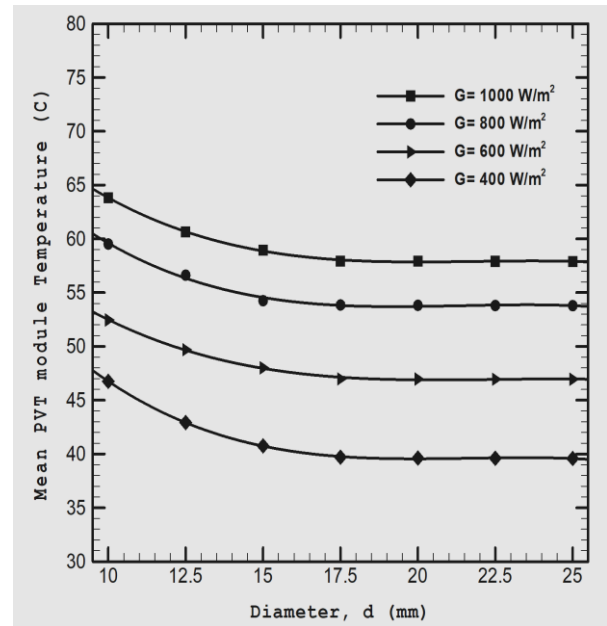


FIGURE 6

T_{PM} VERSUS THE PVT ABSORBER DIMENSIONS (SQUARE TUBE [D]) AT ALTERED SOLAR IRRADIANCE BESIDES MASS FLOWRATE $\dot{m} = 0.068 \text{ KG/S}$

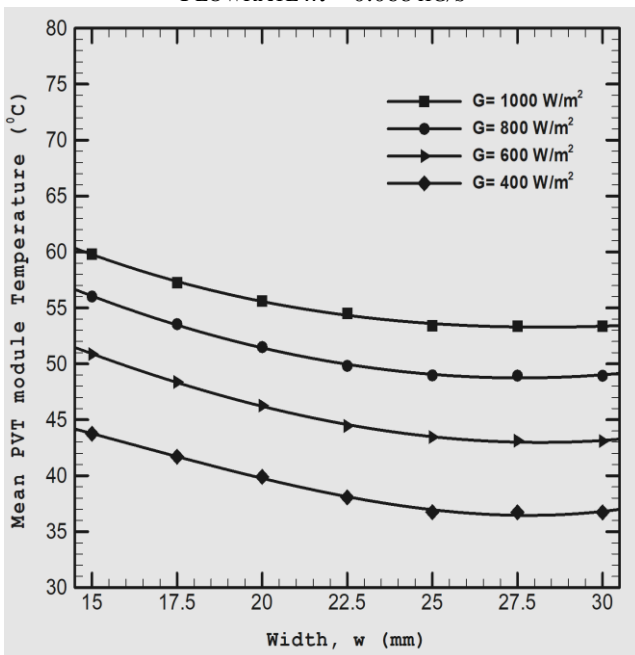


FIGURE 7

T_{PM} VERSUS THE PVT ABSORBER DIMENSIONS (RECTANGULAR TUBE [w], $D = 15 \text{ MM}$) AT ALTERED SOLAR IRRADIANCE BESIDES MASS FLOWRATE $\dot{m} = 0.068 \text{ KG/S}$

4. Performance Evaluation of PV/T Collector Using Round Tube [$d = 15 \text{ mm}$] Base - Fluid (Water)

In the contemporary revision, in order to appraise the current enactment of the Round tube [$d = 15 \text{ mm}$] via aquatic as improper fluid, the outlet temperatures were collected and plotted versus mass flow rates. Figure 8 shows the outlet temperature profile versus mass flow rates ($0.068 - 0.170 \text{ kg/s}$) at solar irradiance ($400, 600, 800$ and 1000 W/m^2). As it is seen in this figure, by increased the mass flow rate the outlet temperature decreases during the all solar irradiance

and it is slightly be constant of decreases at the optimum mass flow rate 0.170 kg/s. At the solar irradiance 1000 W/m² the outlet water temperature dropped from 44.21 °C to 41.26 °C.

Figure 8 illustrate the electrical and thermal PV/T efficiencies, with a mean PV/T module temperature vs. mass flow rate range of (0.0 - 0.170 kg/s) at different solar radiation levels (400, 600, 800, and 1000 W/m²). The results showed that the mean PV/T module temperature (T_{pm}) of the PV/T collector simultaneously dropping at any solar radiation level when the mass flow rate increased. For similar mass flow rates, T_{pm} increased when the solar radiation level increases.

Figure 9 and Table 2 show the mean PV/T module hotness and electrical PV/T competence (η_{el}) versus different mass flow rate kg/s at different solar irradiance for Round tube [$d = 15\text{ mm}$] absorber collector, at mass flow rate from 0 to 0.170 kg/s with stellar irradiance of 400 W/m² indicated malaise dropped from 57.85 °C to 40.82 °C simultaneously increased the electrical PV/T efficiency from 8.52 % to 11.23 %. When the solar irradiance improved to 1000 W/m², the hotness dropped from 89.62 °C to 69.82 °C and the electrical PV/T effectiveness augmented from 5.40 % to 8.78 %. After this, the effect of mass flow rate on the electrical PV/T effectiveness was extracted negligible. This trend of PV efficiency is found to be the same at altered planetary emission stages.

Figures 10 shows the hotness distributions for Round tube [$d = 15\text{ mm}$], it is very vibrant to grasp how the temperatures increased starting the fjord to the vent.

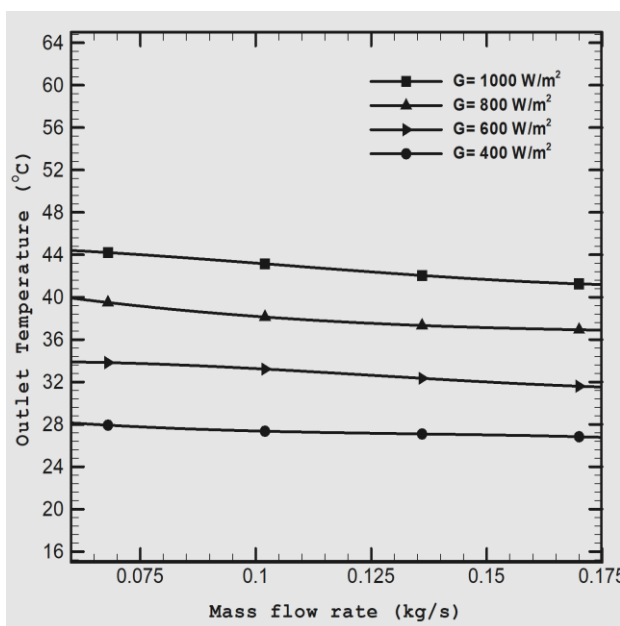


FIGURE 8

OUTLET TEMPERATURE VERSUS DIFFERENT MASS FLOWRATE AT DIFFERENT SOLAR IRRADIANCE FOR ROUND TUBE [$D = 15\text{ MM}$] ABSORBER COLLECTOR

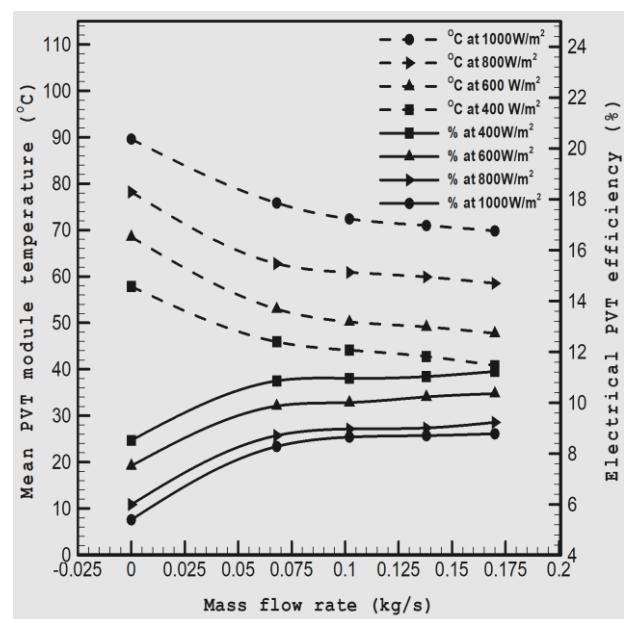


FIGURE 9

T_{PM} WITH η_{EL} VERSUS DIFFERENT MASS FLOW RATE AT DIFFERENT SOLAR IRRADIANCE FOR ROUND TUBE [$D = 15\text{ MM}$] ABSORBER COLLECTOR

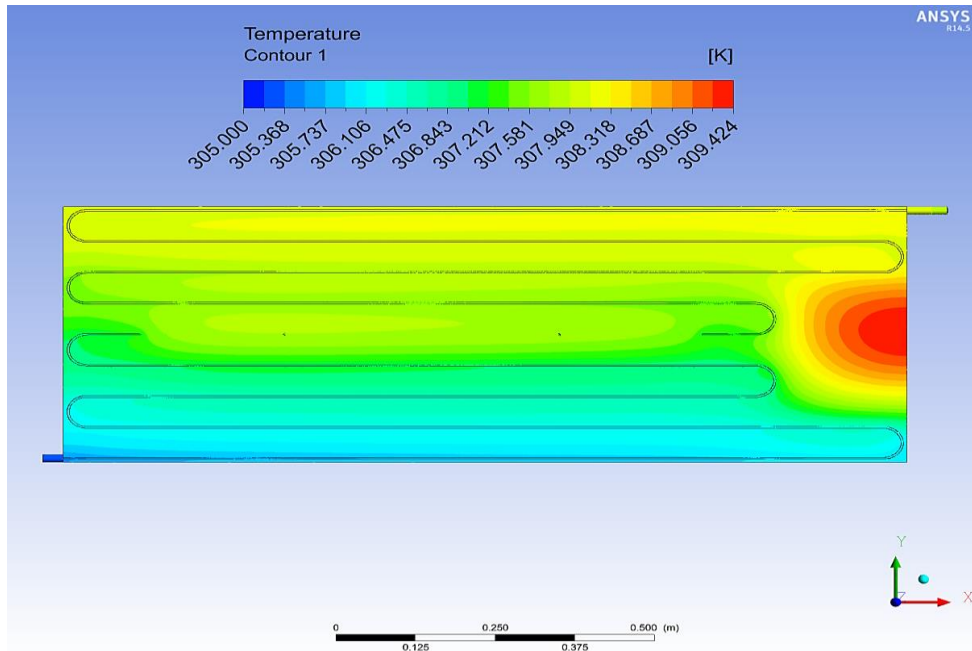


FIGURE 10
TOP SIDE VIEW THE TEMPERATURE DISTRIBUTIONS FOR THE ROUND TUBE [D = 15 MM]

TABLE 2
CHANGE OF η_{EL} OVER T_{PM} FOR ROUND TUBE [D = 15 MM] BELOW NUMEROUS MASS MOVEMENT RATE BESIDES ASTRAL IRRADIANCE

\dot{m} , kg/s	Solar Irradiance							
	400 W/m ²		600 W/m ²		800 W/m ²		1000 W/m ²	
	T_{pm} , °C	η_{el} , %	T_{pm} , °C	η_{el} , %	T_{pm} , °C	η_{el} , %	T_{pm} , °C	η_{el} , %
0	57.85	8.52	68.52	7.52	78.21	6.00	89.62	5.40
0.068	45.92	10.86	52.98	9.87	62.76	8.71	75.84	8.28
0.102	44.12	10.96	50.21	10.01	60.87	8.97	72.41	8.65
0.136	42.76	11.03	49.12	10.23	59.89	9.01	70.98	8.71
0.170	40.82	11.23	47.73	10.36	58.52	9.23	69.82	8.78

5. Performance Evaluation of PV/T Collector Using Round Tube [d = 20 mm] Base - Fluid (Water)

Figure 11 shows the changing of outlet heat contrasted with mass current tariffs at altered lunar irradiance, it is clear to see that, the outlet water temperature dropped when the mass flow rate amplified. At lunar irradiance 1000 W/m² the outlet water heat dropped from 45.83 °C to 42.61 °C for mass flow rate increased from 0.068 kg/s to 0.170 kg/s.

As exposed in Figure 12 and Table 3 the Round tube [d = 20 mm] at mass current degree from 0 kg/s to 0.170 kg/s with solar irradiance of 400 W/m² indicated hotness dropped from 57.85 °C to 37.98 °C simultaneously improved the electrical PV/T effectiveness from 8.52 % to 11.85 %. While the astral irradiance improved to 1000 W/m², the hotness dropped commencing 89.62 °C to 61.52 °C besides the electrical PV/T effectiveness augmented commencing 5.40 % to 9.35 %.

Figures 13 shows the temperature distributions for Round tube [d = 20 mm], it is very vibrant to grasp how the temperatures increased from the inlet to the outlet.

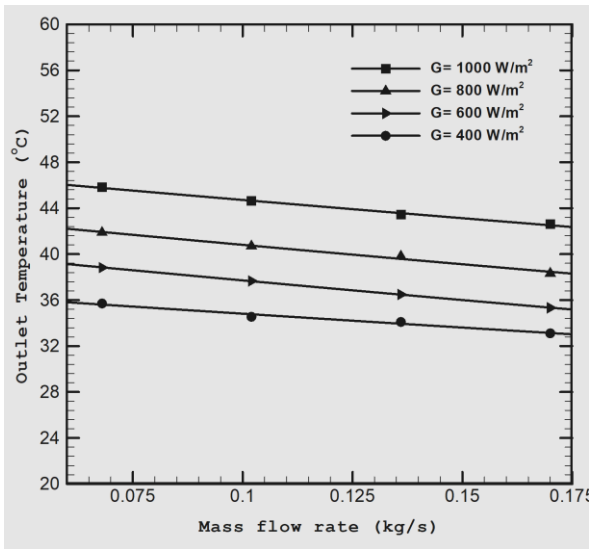


FIGURE 11

OUTLET TEMPERATURE VERSUS DIFFERENT MASS FLOWRATE AT DIFFERENT SOLAR IRRADIANCE FOR ROUND TUBE [D = 20 MM] ABSORBER COLLECTOR

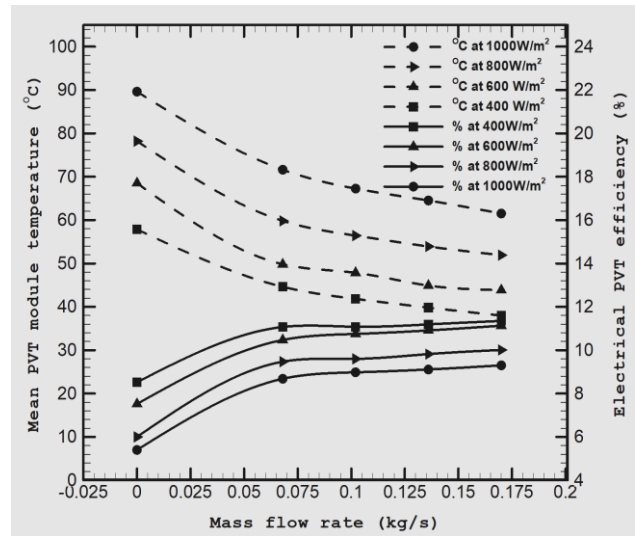


FIGURE 12

TPM AND η_{EL} VERSUS DIFFERENT MASS FLOWRATE AT DIFFERENT SOLAR IRRADIANCE FOR ROUND TUBE [D = 20 MM] ABSORBER COLLECTOR

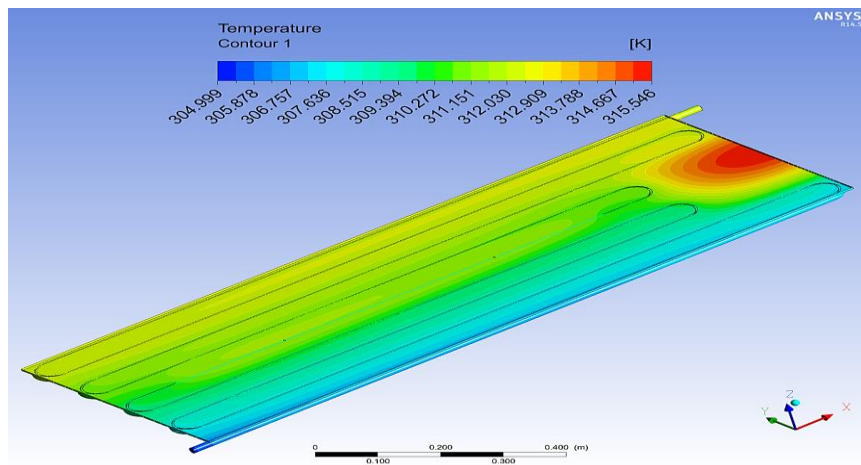


FIGURE 13

3-D DIMENSION THE TEMPERATURE DISTRIBUTIONS FOR THE ROUND TUBE [D = 20 MM]

TABLE 3

CHANGE OF η_{EL} OVER T_{PM} FOR ROUND TUBE [D = 20 MM] UNDER VARIOUS MASS FLOW RATE AND SOLAR IRRADIANCE

\dot{m} , kg/s	Solar Irradiance							
	400 W/m ²		600 W/m ²		800 W/m ²		1000 W/m ²	
	T_{pm} , °C	η_{el} , %	T_{pm} , °C	η_{el} , %	T_{pm} , °C	η_{el} , %	T_{pm} , °C	η_{el} , %
0	57.85	8.52	68.52	7.52	78.21	6.00	89.62	5.40
0.068	44.62	11.07	49.82	10.47	59.82	9.47	71.62	8.68
0.102	41.82	11.08	47.85	10.75	56.42	9.60	67.26	8.98
0.136	39.82	11.19	44.9	10.91	53.91	9.82	64.52	9.11
0.170	37.98	11.85	43.86	11.43	51.92	10.09	61.52	9.35

6. Performance Evaluation of PV/T Collector Using Square Tube [d = 20 mm] Base-Fluid (Water)

Figure 14 shows the changing of outlet hotness versus mass flow rates at different solar irradiance, it is clear to see that, the outlet water temperature dropped when the mass movement rate improved. At solar irradiance 1000 W/m^2 the outlet water hotness dropped from $45.83 \text{ }^\circ\text{C}$ to $43.82 \text{ }^\circ\text{C}$ for mass flow rate increased from 0.068 kg/s to 0.170 kg/s . As exposed in Figure 15 and Table 4 the Square tube [d = 20 mm] at mass flow rate from 0 kg/s to 0.170 kg/s with planetary irradiance of 1000 W/m^2 indicated heat dropped from $89.62 \text{ }^\circ\text{C}$ to $55.85 \text{ }^\circ\text{C}$ simultaneously amplified the electrical PV/T competence from 5.40% to 9.19% . When the stellar irradiance improved to 400 W/m^2 , the hotness dropped from $57.85 \text{ }^\circ\text{C}$ to $31.74 \text{ }^\circ\text{C}$ and the electrical PV/T competence improved from 8.52% to 12.16% . Figures 16 shows the temperature distributions for Square tube [d = 20 mm], it is very perfect to see how the temperatures increased from the fjord to the vent.

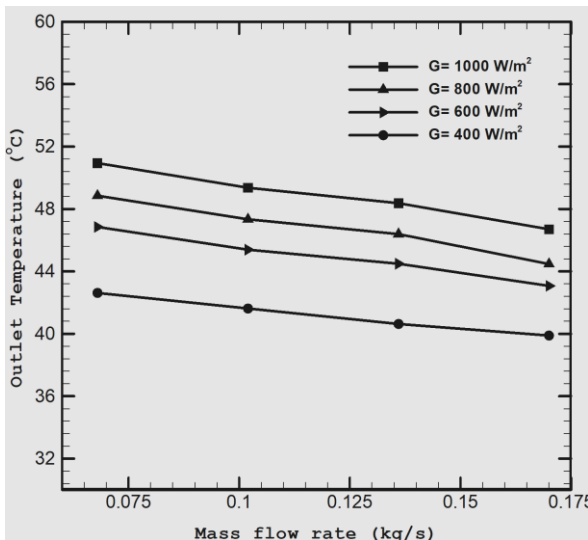


FIGURE 14

OUTLET TEMPERATURE VERSUS DIFFERENT MASS FLOWRATE AT DIFFERENT SOLAR IRRADIANCE FOR SQUARE TUBE [D = 20 MM] ABSORBER COLLECTOR

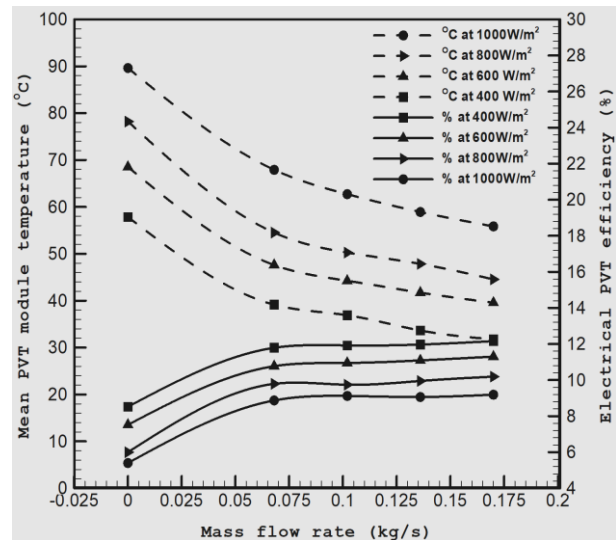


FIGURE 15

TPM AND η_{EL} VERSUS DIFFERENT MASS FLOWRATE AT DIFFERENT SOLAR IRRADIANCE FOR SQUARE TUBE [D = 20 MM] ABSORBER COLLECTOR

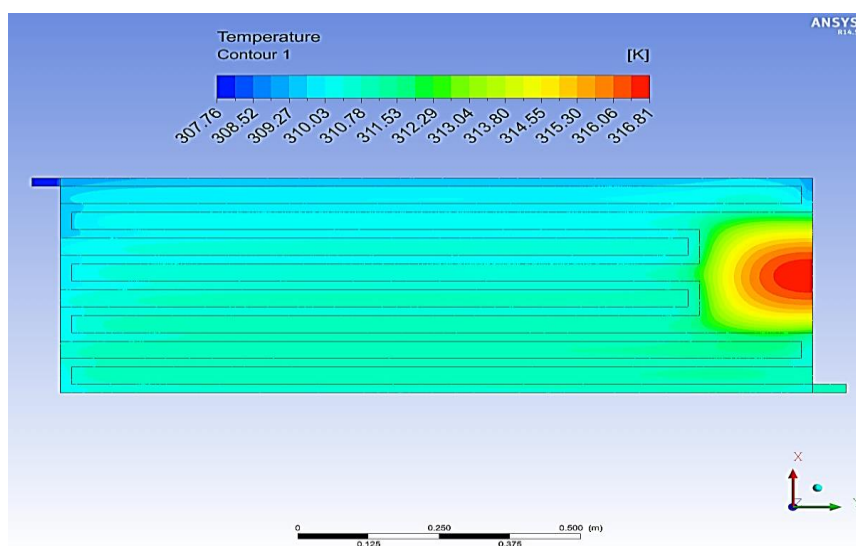


FIGURE 16

TOP SIDE VIEW THE TEMPERATURE DISTRIBUTIONS FOR THE SQUARE TUBE [D = 20 MM]

TABLE 4

CHANGE OF η_{EL} OVER T_{PM} FOR SQUARE TUBE [D = 20 MM] UNDER VARIOUS MASS FLOW RATE AND SOLAR IRRADIANCE

\dot{m} , kg/s	Solar Irradiance							
	400 W/m ²		600 W/m ²		800 W/m ²		1000 W/m ²	
	T_{pm} , °C	η_{el} , %	T_{pm} , °C	η_{el} , %	T_{pm} , °C	η_{el} , %	T_{pm} , °C	η_{el} , %
0	57.850	8.520	68.520	7.520	78.210	6.000	89.620	5.400
0.680	39.150	11.790	47.620	10.770	54.520	9.790	67.921	8.870
0.102	36.900	11.920	44.250	10.950	50.260	9.740	62.720	9.120
0.136	33.650	11.970	41.720	11.090	47.850	9.950	58.920	9.060
0.170	31.740	12.160	39.560	11.300	44.550	10.190	55.850	9.190

7. Performance Evaluation of PV/T Collector Using Rectangular Tube [w = 25 mm, d = 15 mm] (Water)

Based - Fluid

Figure 17 illustrate the changing of outlet hotness as opposed to mass movement tariffs at different solar irradiance, it is clear to see that, the outlet water temperature dropped when the mass flow rate increased. At solar irradiance 1000 W/m² the outlet water temperature dropped from 52.78 °C to 49.57 °C for mass flow rate increased from 0.068 kg/s to 0.170 kg/s. As shown in Figure 18 and Table 5 the Rectangular tube [w = 25 mm, d = 15 mm] at mass flow rate from 0 kg/s to 0.170 kg/s with stellar irradiance of 1000 W/m² indicated hotness dropped from 89.62 °C to 50.32 °C simultaneously improved the electrical PV/T efficiency from 5.40 % to 9.60 %. When the solar irradiance improved to 400 W/m², the temperature dropped from 57.85 °C to 29.98 °C and the electrical PV/T efficiency improved from 8.52 % to 12.45 %.

Figures 19 indication the temperature distributions to Rectangular tube [w = 25 mm, d = 15 mm], it is very perfect to grasp how the temperatures increased since the fjord to the vent.

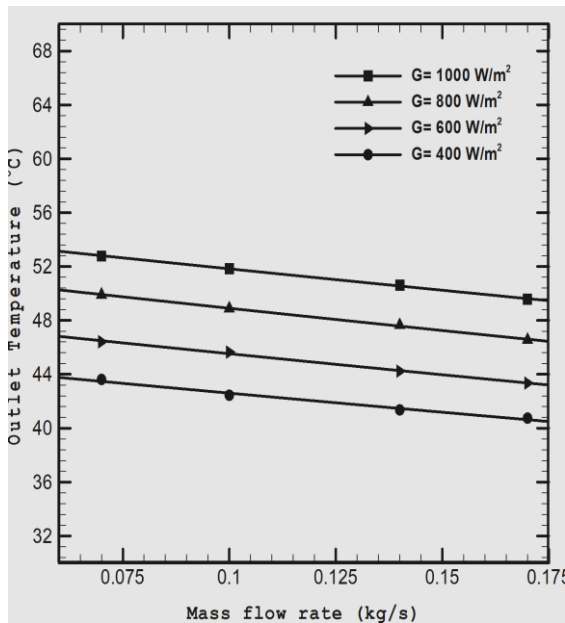


FIGURE 17

OUTLET TEMPERATURE VERSUS DIFFERENT MASS FLOW RATE AT DIFFERENT SOLAR IRRADIANCE FOR RECTANGULAR TUBE [w = 25 MM, D = 15 MM] ABSORBER COLLECTOR

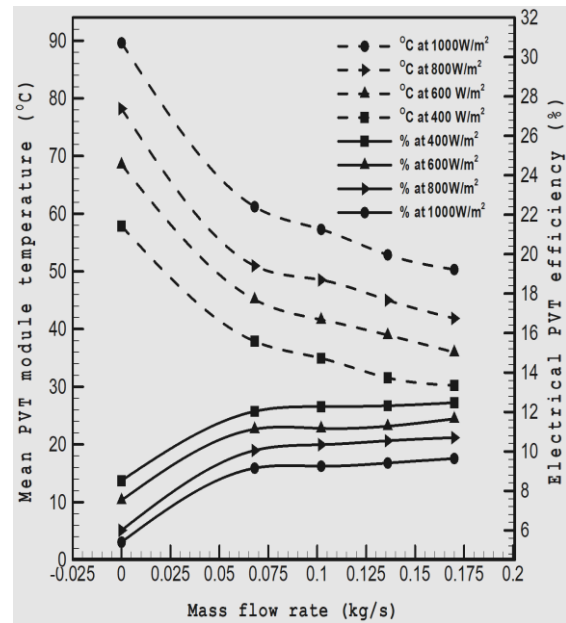


FIGURE 18

T_{PM} AND η_{EL} VERSUS DIFFERENT MASS FLOWRATE AT DIFFERENT SOLAR IRRADIANCE FOR RECTANGULAR TUBE [w = 25 MM, D = 15 MM] ABSORBER COLLECTOR

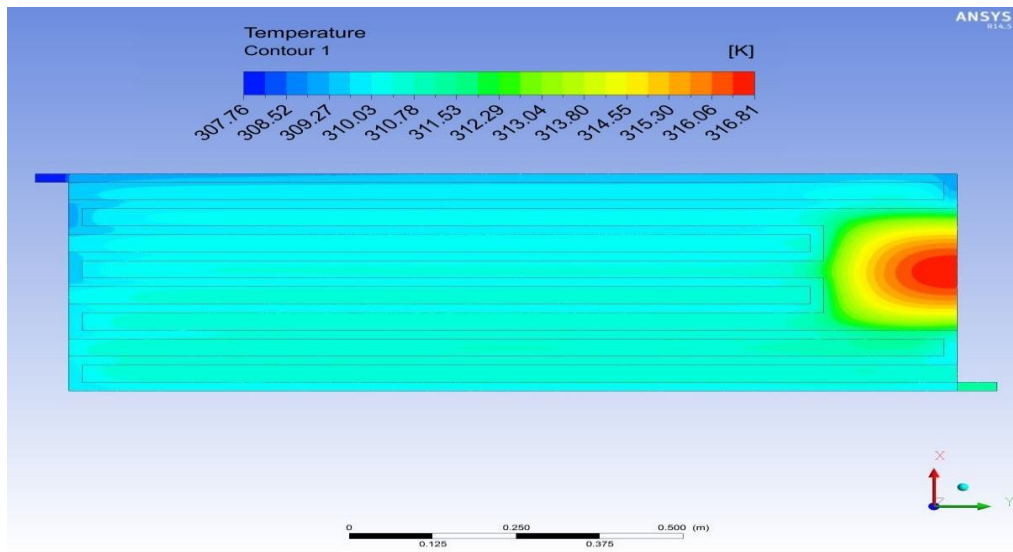


FIGURE 19
TOP SIDE VIEW THE TEMPERATURE DISTRIBUTIONS FOR THE RECTANGULAR TUBE [w = 25 MM, D = 15 MM]

TABLE 5
CHANGE OF η_{EL} OVER T_{PM} FOR RECTANGULAR TUBE [w = 25 MM, D = 15 MM] UNDER VARIOUS MASS FLOW RATE AND SOLAR IRRADIANCE

\dot{m} , kg/s	Solar Irradiance							
	400 W/m ²		600 W/m ²		800 W/m ²		1000 W/m ²	
	T_{pm} , °C	η_{el} , %	T_{pm} , °C	η_{el} , %	T_{pm} , °C	T_{pm} , °C	η_{el} , %	
0	57.85	8.52	68.52	7.52	78.21	6.00	89.62	5.40
0.068	35.74	12.03	45.12	11.17	50.97	9.88	62.54	9.15
0.102	35.02	12.27	41.63	11.17	48.52	10.14	57.62	9.25
0.136	31.26	12.33	38.95	11.25	45.01	10.54	52.47	9.41
0.170	29.98	12.45	35.98	11.60	41.85	10.63	50.32	9.60

8. Recital Assessment of PV/T Gatherer Using Rectangular Tube [w = 25 mm, d = 15 mm] Based - Fluid (Water)

The numerical recital of PV/T collector can be depicted by the combination of competence appearance. It embraced of the thermal PV/T competence (η_{th}) and electrical PV/T competence (η_{el}), these efficiencies typically include of the beneficial current improvement besides electrical improvement of the scheme. The total of the efficiencies, which is known as overall efficiency ($\eta_{overall}$), is used to evaluate the overall numerical performance of the scheme. Based on the CFD numerical analysis on the PV/T collectors, it is proved that both efficiencies increased when the mass flow rate increased. Therefore, the PV/T overall efficiency increased concurrently when the mass flow rate increased. The numerical results of electrical PV/T efficiency (η_{el}), thermal PV/T efficiency ($\eta_{thermal}$), and overall PV/T efficiency ($\eta_{overall}$) over mass flow rates for PV/T collectors at solar irradiance 1000 W/m² can be seen as in Figure 20 to Figure 21. For the η_{el} over mass flow rate as shown in Figure 20, it is clear to see that the electrical efficiency increased and enhanced for all the PV/T collectors designs compare with the reference PV module only efficiency. For the $\eta_{thermal}$ over mass movement proportion as exposed in Figure 21, it is clear to see that the thermal competence augmented and enhanced for all the PV/T gatherers designs. Finally For the overall PV/T efficiency ($\eta_{overall}$) over mass flow rate as exposed in Figure 22, it is clear to see that the overall competence increased and enhanced for totally the PV/T collectors designs. The highest and best numerical enhancement for competences were found to Rectangular tube [w = 25 mm, d = 20 mm] the $\eta_{overall}$ increased from 67.57 % to 73.40 %, followed by Rectangular tube [d = 20 mm] increased from 65.71 % to 71.00 %, Round tube [d = 20 mm] increased from 61.25 % to 66.92 %, and Round tube [d = 15 mm] increased from 59.35 % to 65.06 % respectively.

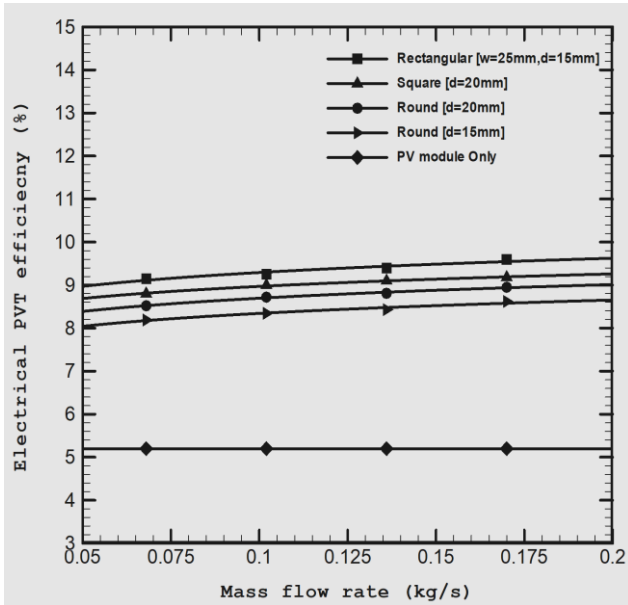


FIGURE 20

THE η_{EL} OVER MASS FLOW RATES FOR PVT COLLECTORS AT SOLAR IRRADIANCE OF 1000 W/M^2

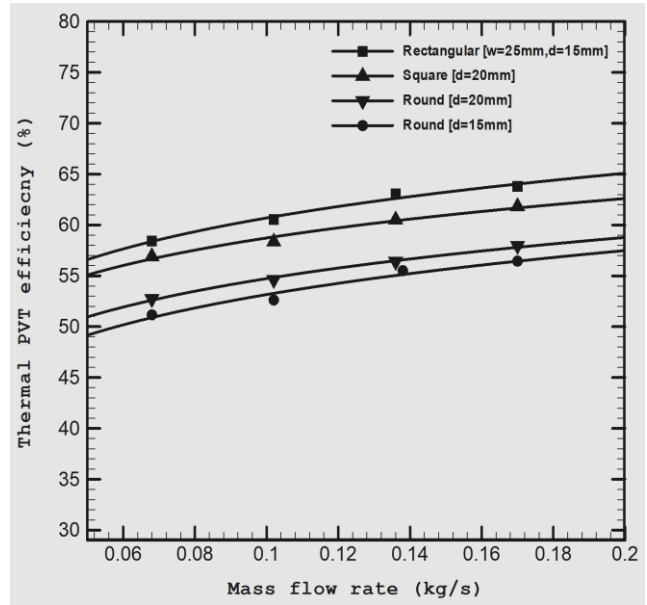


FIGURE 21

THE η_{TH} FOR THE PVT COLLECTOR OVER VARIOUS MASS FLOW RATES AT SOLAR IRRADIANCE OF 1000 W/M^2

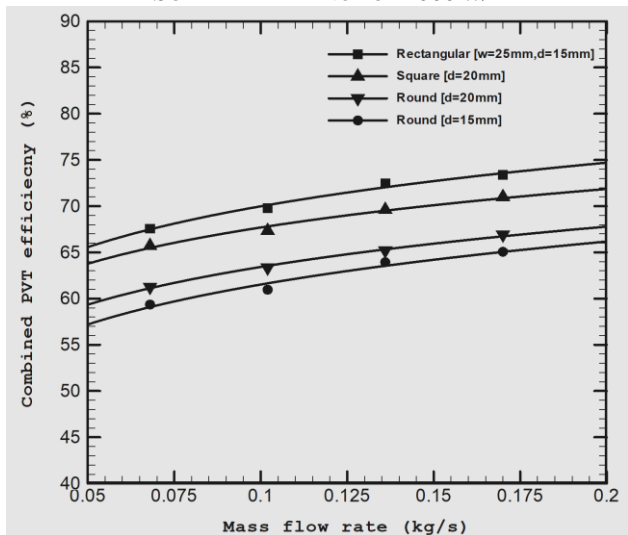


FIGURE 22

THE $\eta_{OVERALL}$ FOR THE PVT COLLECTOR OVER VARIOUS MASS FLOW RATES AT SOLAR IRRADIANCE OF 1000 W/M^2

CONCLUSIONS

This revision investigated the optimum design and absorber configurations of photovoltaic thermal collector using three types of tubes are used in these designs (Round tube, Square tube and Rectangular tube). The results shown that the major contributors to the best of the absorber collectors design are contributed by the design configuration, the argument factors that contributed the design configuration is Rectangular tube [$w = 25 \text{ mm}$, $d = 15 \text{ mm}$] giving higher enhancement with overall PV/T efficiency 73.40 % compared to the Round tubes shape due to the flat surface contacting underneath the PV module.

NOMENCLATURE

A_c Function of the gatherer part (m^2)

C_p Precise emotion of the collector cooling medium ($J/kg K$)
 F_R Emotion elimination efficiency element
 h_{fi} Hotness allocation measurement of fluid ($W/m^2 K$)
 W Tube spacing (m)
 U_L Global gatherer hotness defeat measurement ($W/m^2 K$)
 τ Transmissivity
 α Absorptivity
 μ Dynamic viscosity of the fluid (mPa.s)
 η_{el} Electrical efficiency (%)
 η_{th} Thermal PVT efficiency (%)

REFERENCES

- [1] Abbud, L.H., Balla, H.H., Abdulwahid, A.F., & Karim, Z.S., "Study of Thermal and Mechanical Properties of Fiberglass Multi-Wall Carbon Nanotube/Epoxy," *Frontiers in Heat and Mass Transfer*, Vol. 13, 2019.
- [2] Al-Shamani, A.N., Mat, S., Ruslan, M.H., Abed, A.M., & Sopian, K., "Numerical study on the characteristics of a specially designed rectangular tube absorber photovoltaic thermal collector (PVT)," *WSEAS Transactions on Environment and Development*, Vol. 11, 2015, pp. 23-28.
- [3] Al-Shamani, A.N., Yazdi, M.H., Alghoul, M.A., Abed, A.M., Ruslan, M.H., Mat, S., & Sopian, K., "Nanofluids for improved efficiency in cooling solar collectors—a review," *Renewable and Sustainable Energy Reviews*, Vol. 38, 2014, pp. 348-367.
- [4] Bergene, T., & Løvvik, O.M., "Model calculations on a flat-plate solar heat collector with integrated solar cells," *Solar Energy*, Vol. 55, No. 6, 1995, pp. 453-462.
- [5] Chow, T., "Performance analysis of photovoltaic-thermal collector by explicit dynamic model," *Solar Energy*, Vol. 75, No. (2), 2003, pp. 143-152.
- [6] Coventry, J.S., "Performance of a concentrating photovoltaic/thermal solar collector," *Solar Energy*, Vol. 78, No. 2, 2005, pp. 211-222.
- [7] Cox lli, C., & Raghuraman, P., "Design considerations for flat-plate-photovoltaic/thermal collectors," *Solar Energy*, Vol. 35, No. 3, 1985, pp. 227-241.
- [8] Duffie, J.A., & Beckman, W.A., "Solar engineering of thermal processes," John Wiley & Sons, 2013.
- [9] Eiamsa-ard, S., & Promvonge, P., "Numerical study on heat transfer of turbulent channel flow over periodic grooves," *International Communications in Heat and Mass Transfer*, Vol. 35, No. 7, 2008, pp. 844-852.
- [10] Fudholi, A., Sopian, K., Yazdi, M.H., Ruslan, M.H., Ibrahim, A., & Kazem, H.A., "Performance analysis of photovoltaic thermal (PVT) water collectors," *Energy conversion and management*, Vol. 78, 2014, pp. 641-651.
- [11] Ibrahim, A., Othman, M.Y., Ruslan, M.H., Alghoul, M., Yahya, M., Zaharim, A., & Sopian, K., "Performance of photovoltaic thermal collector (PVT) with different absorbers design," *WSEAS Transactions on Environment and Development*, Vol. 5, No. 3, 2009, pp. 321-330.
- [12] Jedsadaratanachai, W., & Boonloi, A., "Thermal performance improvement in a square channel heat exchanger with various parameters of v-wavy plates," *Frontiers in Heat and Mass Transfer (FHMT)*, 2018.
- [13] Joshi, A.S., Tiwari, A., Tiwari, G.N., Dincer, I., & Reddy, B.V., "Performance evaluation of a hybrid photovoltaic thermal (PV/T)(glass-to-glass) system," *International Journal of Thermal Sciences*, Vol. 48, No. 1, 2009, pp. 154-164.
- [14] Mbewe, D.J., Card, H.C., & Card, D.C., "A model of silicon solar cells for concentrator photovoltaic and photovoltaic/thermal system design," *Solar energy*, Vol. 35, No. 3, 1985, pp. 247-258.
- [15] Moradi, K., Ebadian, M.A., & Lin, C.X., "A review of PV/T technologies: Effects of control parameters," *International journal of heat and mass transfer*, Vol. 64, 2013, pp. 483-500.
- [16] Ndlovu, P., & Moitsheki, R. Thermal analysis of natural convection and radiation heat transfer in moving porous fins. *Frontiers in Heat and Mass Transfer (FHMT)*, 2018.
- [17] Sapit, A. B., & Pahat, B., "Experimental Investigation of Thermal Performance of Backflow Corrugated Solar Air Heater Collector Integrated with Phase Change Material (PCM)," *Jour of Adv Research in Dynamical & Control Systems*, Vol. 11, No. 6, 2019, pp. 17-39.
- [18] Sarhaddi, F., Farahat, S., Ajam, H., Behzadmehr, A.M.I.N., & Adeli, M.M., "An improved thermal and electrical model for a solar photovoltaic thermal (PV/T) air collector," *Applied energy*, Vol. 87, No. 7, 2010, pp. 2328-2339.
- [19] Skoplaki, E., & Palyvos, J.A., "On the temperature dependence of photovoltaic module electrical performance: A review of efficiency/power correlations," *Solar Energy*, Vol. 83, No. (5), 2009, pp. 614-624.
- [20] Sok, E., "Performance and economic evaluation of a hybrid photovoltaic/thermal solar scheme in Northern China," *International Journal of Energy and Power Engineering*, Vol. 4, No. 12, 2010, pp. 1738-1743.
- [21] Takashima, T., Tanaka, T., Doi, T., Kamoshida, J., Tani, T., & Horigome, T., "New proposal for photovoltaic-thermal solar energy utilization method," *Solar energy*, Vol. 52, No. 3, 1994, pp. 241-245.
- [22] Tiwari, A., & Sodha, M., "Performance evaluation of hybrid PV/thermal water/air heating scheme: a parametric study," *Renewable energy*, Vol. 31, No. 15, 2006, pp. 2460-2474.
- [23] Tripanagnostopoulos, Y., "Aspects and improvements of hybrid photovoltaic/thermal solar energy schemes," *Solar Energy*, Vol. 81(9), 2007, pp. 1117-1131.

- [24] Zarita, R., & Hachemi, M, "Numerical investigation and analysis of heat transfer enhancement in a microchannel using nanofluids by the lattice Boltzmann method," *Frontiers in Heat and Mass Transfer (FHMT)*, 2018.
- [25] Zhong, Y., & Ling, C, "Effects of Serrated Pulsating Airflow on Liquid Film Evaporation in A Vertical Channel: a Numerical Study," *Frontiers in Heat and Mass Transfer (FHMT)*, 2020.
- [26] Zondag, H, "Flat-plate PV-Thermal collectors and schemes: A review," *Renewable and Sustainable Energy Reviews*, Vol. 12, No. 4, 2008, pp. 891-959.
- [27] Zondag, H.A., Jong, M.J., & Helden, W.G.J, "Development and applications for PV thermal," Energy research Centre of the Netherlands ECN, 2001.